



Fermi National Accelerator Laboratory

FERMILAB-Pub-93/331-E  
E761

# $P_t$ and $X_F$ Dependence of the Polarization of $\Sigma^+$ Hyperons Produced by 800 GeV/c Protons

A. Morelos et al  
The E761 Collaboration

*Fermi National Accelerator Laboratory, P.O. Box 500, Batavia, Illinois 60510*  
*Petersburg Nuclear Physics Institute, Gatchina, Russia*  
*Institute of High Energy Physics, Beijing, PRC*  
*H.H. Wills Physics Laboratory, University of Bristol, UK*  
*Carnegie Mellon University, Pittsburgh, PA 15213*  
*University of Iowa, Iowa City, IA 52242*  
*Institute of Theoretical and Experimental Physics, Moscow, Russia*  
*State University of New York at Albany, Albany NY 12222*  
*Universidade Federal da Paraiba, Paraiba, Brazil*  
*Centro Brasileiro de Pesquisas Fisicas, Rio de Janeiro, Brazil*  
*Conselho Nacional de Pesquisas CNPq, Rio de Janeiro, Brazil*  
*Universidade de Sao Paulo, Sao Paulo, Brazil*  
*J.W. Gibbs Laboratory, Yale University, New Haven CT 06511*

November 1993

Submitted to *Physical Review Letters*

## **Disclaimer**

*This report was prepared as an account of work sponsored by an agency of the United States Government. Neither the United States Government nor any agency thereof, nor any of their employees, makes any warranty, express or implied, or assumes any legal liability or responsibility for the accuracy, completeness, or usefulness of any information, apparatus, product, or process disclosed, or represents that its use would not infringe privately owned rights. Reference herein to any specific commercial product, process, or service by trade name, trademark, manufacturer, or otherwise, does not necessarily constitute or imply its endorsement, recommendation, or favoring by the United States Government or any agency thereof. The views and opinions of authors expressed herein do not necessarily state or reflect those of the United States Government or any agency thereof.*

# **$P_t$ and $X_F$ Dependence of the Polarization of $\Sigma^+$ Hyperons Produced By 800 GeV/c Protons**

A.Morelos<sup>1(a)</sup>, I.F.Albuquerque<sup>6(b)</sup>, N.F.Bondar<sup>3</sup>, R.Carrigan Jr.<sup>1</sup>,  
D.Chen<sup>10(c)</sup>, P.S.Cooper<sup>1</sup>, Dai Lisheng<sup>2</sup>, A.S.Denisov<sup>3</sup>, A.V.Dobrovolsky<sup>3</sup>,  
T.Dubbs<sup>5(d)</sup>, A.M.F.Endler<sup>8</sup>, C.O.Escobar<sup>6</sup>, M.Foucher<sup>7(e)</sup>,  
V.L.Golovtsov<sup>3</sup>, H.Gottschalk<sup>1(f)</sup>, P.Gouffon<sup>6(g)</sup>, V.T.Grachev<sup>3</sup>,  
A.V.Khanzadeev<sup>3</sup>, M.A.Kubantsev<sup>4</sup>, N.P.Kuropatkin<sup>3</sup>, J.Lach<sup>1</sup>,  
Lang Pengfei<sup>2</sup>, V.N.Lebedenko<sup>4</sup>, Li Chengze<sup>2</sup>, Li Yunshan<sup>2</sup>, M.Luksys<sup>13(h)</sup>,  
J.R.P.Mahon<sup>6(g)</sup>, E.McCliment<sup>5</sup>, C.Newsom<sup>5</sup>, M.C.Pommot Maia<sup>9(i)</sup>,  
V.M.Samsonov<sup>3</sup>, V.A.Schegelsky<sup>3</sup>, Shi Huanzhang<sup>2</sup>, V.J.Smith<sup>11</sup>,  
Tang Fukun<sup>2</sup>, N.K.Terentyev<sup>3</sup>, S.Timm<sup>12</sup>, I.I.Tkatch<sup>3</sup>, L.N.Uvarov<sup>3</sup>,  
A.A.Vorobyov<sup>3</sup>, Yan Jie<sup>2</sup>, Zhao Wenheng<sup>2</sup>, Zheng Shuchen<sup>2</sup>,  
Zhong Yuanyuan<sup>2</sup>

(1) Fermi National Accelerator Laboratory, Batavia, IL60510

(2) Institute of High Energy Physics, Beijing, PRC

(3) St. Petersburg Nuclear Physics Institute, Gatchina, Russia

(4) Institute of Theoretical and Experimental Physics, Moscow, Russia

(5) University of Iowa, Iowa City, IA 52242

(6) Universidade de Sao Paulo, Sao Paulo, Brazil

(7) J.W. Gibbs Laboratory, Yale University, New Haven, CT 06511

(8) Centro Brasileiro de Pesquisas Fisicas, Rio de Janeiro, Brazil

(9) Conselho Nacional de Pesquisas CNPq, Rio de Janeiro, Brazil

(10) State University of New York at Albany, Albany, NY 12222

(11) H.H. Wills Physics Laboratory, University of Bristol, UK

(12) Carnegie Mellon University, Pittsburgh, PA 15213

(13) Universidade Federal da Paraiba, Paraiba, Brazil

(E761 Collaboration)

November 3, 1993

We utilize the excellent angle and momentum resolution of our apparatus to study the polarization of 375 GeV/c  $\Sigma^+$  hyperons produced by 800 GeV/c protons incident on a Cu target. By examining in detail two of our high statistics data points, we find evidence for structure in the  $p_t$  dependence of  $\Sigma^+$  polarization and are able to extract the  $X_F$  dependence of the  $\Sigma^+$  polarization and compare it with  $X_F$  behavior in the  $\Lambda^0$  and  $\Xi^-$  systems.

PACS numbers: 13.85.Ni, 13.88.+e

Information on the kinematical dependence of the polarization is an important test of theoretical hyperon production models. In this article we

extract new information available in the high statistics data points which formed the basis of a previous letter<sup>1</sup>. Studying the dependence of the polarization within each data point yields new information on the detailed structure of the of  $P_{\uparrow}$  and  $X_F$  dependence of the polarization of inclusively produced  $\Sigma^+$  hyperons.

Although each of the data points corresponds to only one setting of the E761 spectrometer, each includes data in a finite range of  $P_{\uparrow}$  and  $X_F$  corresponding to the angular and momentum acceptance of the hyperon channel<sup>2</sup> and spectrometer. For points containing a large number of events, we have the sensitivity to extract information on the  $P_{\uparrow}$  and  $X_F$  dependence of the  $\Sigma^+$  polarization within that data point.

The horizontal (H) targeting angle data<sup>1</sup> at  $\pm 3.7$  mrad include over twelve million events and were used to measure the asymmetry parameter<sup>3</sup> in the  $\Sigma^+ \rightarrow p\gamma$  radiative decay. Vertical (V) targeting angle data at  $\pm 2.9$  mrad containing about a quarter million events were taken as part of a measurement of the  $\Sigma^+$  magnetic moment<sup>4</sup>. Our analysis rests on our understanding of the acceptance of our spectrometer to incident  $\Sigma^+$  in the full range of our beam phase space. Comparing the polarizations at two nominally equal and opposite targeting angles allows us to measure the mean polarization with well controlled precision. However, the beam phase space distributions are not identical for these two complementary angles and if we divide the events of a particular spectrometer setting into bins of equal  $P_{\uparrow}$  or  $X_F$  we must take this into account. To do this requires a large event sample. The 3.7 mrad and vertical points contains such a samples.

The 3.7 mrad horizontal sample and the vertical targeting sample were divided into 7 and 6 bins in  $P_{\uparrow}$  respectively. The  $\Sigma^+$  polarization was computed for each of the bins and is shown in Table I and displayed in Figure 1 with the other E761  $\Sigma^+$  polarization data<sup>1,5</sup>. Table I displays both the statistical and systematic uncertainty of the polarization for these points. Note that the statistical uncertainty of the polarization depends not just on the total number of events in the data bin but also how they are divided among the two complementary targeting angles. The mean values of  $X_F$  ( $P_{\uparrow}$ ) for the two targeting angles are shown in Table I (II). These indicate the differences in the beam phase space

TABLE I. Polarization in bins of  $P_t$ . The values of  $X_F$  of positive and negative targeting angles are shown as  $X_{F+}$  and  $X_{F-}$  respectively. The polarization errors are statistical and systematic respectively.

Angle [mrad]	events	$X_{F+}$	$X_{F-}$	$\langle P_t \rangle$ [GeV/c]	Polarization
0.9 H	14,134	0.463	0.483	0.35	$0.106 \pm 0.015 \pm 0.032$
2.9 V	86,480	0.445	0.445	0.85	$0.171 \pm 0.006 \pm 0.006$
2.9 V	237,087	0.455	0.455	0.95	$0.177 \pm 0.004 \pm 0.006$
2.9 V	204,625	0.465	0.465	1.05	$0.166 \pm 0.004 \pm 0.006$
2.9 V	136,187	0.475	0.475	1.15	$0.153 \pm 0.005 \pm 0.006$
2.9 V	69,990	0.485	0.485	1.25	$0.123 \pm 0.007 \pm 0.006$
2.9 V	14,684	0.495	0.495	1.35	$0.139 \pm 0.014 \pm 0.006$
3.3 H	20,351	0.463	0.483	1.24	$0.131 \pm 0.012 \pm 0.032$
3.7 H	227,055	0.442	0.518	1.19	$0.117 \pm 0.006 \pm 0.003$
3.7 H	808,435	0.448	0.508	1.25	$0.117 \pm 0.002 \pm 0.003$
3.7 H	2,013,063	0.456	0.496	1.31	$0.126 \pm 0.001 \pm 0.003$
3.7 H	2,962,453	0.461	0.488	1.37	$0.124 \pm 0.001 \pm 0.003$
3.7 H	2,785,141	0.467	0.478	1.43	$0.124 \pm 0.001 \pm 0.003$
3.7 H	1,813,897	0.473	0.468	1.49	$0.120 \pm 0.001 \pm 0.003$
3.7 H	946,869	0.479	0.457	1.55	$0.121 \pm 0.002 \pm 0.003$
3.8 H	43,225	0.463	0.483	1.40	$0.112 \pm 0.011 \pm 0.032$
4.3 H	23,173	0.463	0.483	1.64	$0.112 \pm 0.011 \pm 0.032$
4.8 H	23,744	0.463	0.483	1.80	$0.104 \pm 0.011 \pm 0.032$

when the targeting angle is reversed. Our analysis technique yields the arithmetic average of the polarization at the two targeting angle viz:

$$P(P_t) = 1/2[P(X_{F+}, P_t) + P(X_{F-}, P_t)].$$

In the analysis of reference 1 all events were subjected to a restriction that the proton be well away from the walls of the photon calorimeter hole. Figure 2a of reference 1 shows the event mass distribution with this selection imposed. The number of events and range of  $P_t$  coverage in the vertical targeting sample can be increased significantly if we relax this restriction. The vertical targeting sample without this criteria is shown in Tables I and II. All horizontal data points retain this cut.

The systematic uncertainties are estimated from variations of our selection criteria in decay angle, decay vertex position, and missing mass. For the vertical targeting point, releasing the calorimeter edge restriction increases the  $P_t$  coverage significantly; however, this also increases the mean polarization by  $0.0090 \pm 0.0045$  where the error is our estimate of the systematic uncertainty. This value is used to correct all bins of the vertical targeting sample. This and the other systematic uncertainties were combined in quadrature and are also given in Table I and Figure 1. An overall scale uncertainty due to the error<sup>6</sup> in the determination of the  $\alpha$  parameter of 1.6% is not included.

In Figure 1 we note that from the vertical targeting point alone the polarization reaches a maximum near  $P_t = 1$  GeV/c. The inclusion of the 3.7 mrad sample data points confirms that the polarization has decreased by ~25% from  $P_t = 1.0$  to  $P_t = 1.4$  GeV/c and the rate of decrease has become less. QCD predicts<sup>7</sup> that the polarization should vanish at large  $P_t$  and rotational invariance requires that it be zero at  $P_t = 0$ . However, vanishing at zero and large  $P_t$  does not preclude complex behavior in intermediate  $P_t$  regions.

We choose to divide the event samples in these two high statistics points in equal bins of  $X_F$  and study the  $X_F$  dependence of  $\Sigma^+$  polarization for two different values of  $P_t$ . This is shown in Table II and displayed in Figure 2a for each of these samples. In each case we see the polarization increasing with  $X_F$ . These distributions have been fitted to a straight line whose slope ( $dP/dX_F$ ) indicates the change of polarization as a function of  $X_F$ . The fitted values of  $dP/dX_F$  are given in Table III.

TABLE II. Polarization in bins of  $X_F$ . The values of  $P_t$  of positive and negative targeting angles are shown as  $P_{t+}$  and  $P_{t-}$  respectively. The polarization errors are statistical and systematic respectively.

Angle [mrad]	Events	$P_{t+}$ [GeV/c]	$P_{t-}$ [GeV/c]	$X_F$	Polarization
2.9 V	5,087	1.02	1.02	0.445	$0.116 \pm 0.026 \pm 0.003$
2.9 V	38,077	1.04	1.04	0.455	$0.147 \pm 0.010 \pm 0.003$
2.9 V	79,080	1.07	1.07	0.465	$0.157 \pm 0.007 \pm 0.003$
2.9 V	77,284	1.09	1.09	0.475	$0.169 \pm 0.007 \pm 0.003$
2.9 V	40,579	1.11	1.11	0.485	$0.171 \pm 0.009 \pm 0.003$
2.9 V	9,174	1.13	1.13	0.495	$0.199 \pm 0.020 \pm 0.003$
3.7 H	1,206,016	1.33	1.46	0.455	$0.125 \pm 0.002 \pm 0.003$
3.7 H	1,872,136	1.37	1.45	0.461	$0.117 \pm 0.002 \pm 0.003$
3.7 H	2,249,978	1.41	1.43	0.467	$0.118 \pm 0.001 \pm 0.003$
3.7 H	2,166,507	1.45	1.42	0.473	$0.126 \pm 0.001 \pm 0.003$
3.7 H	1,773,641	1.49	1.40	0.479	$0.122 \pm 0.001 \pm 0.003$
3.7 H	1,278,412	1.53	1.39	0.485	$0.128 \pm 0.002 \pm 0.003$
3.7 H	811,293	1.57	1.37	0.491	$0.136 \pm 0.003 \pm 0.003$

In order to attempt an understanding of the polarization mechanism, comparison with other hyperons is important. Hyperon production polarization data with 400 GeV incident protons exists in a similar kinematical region for the  $\Lambda^0$  system<sup>8</sup>. Even though these data extend out to much larger values of  $P_t$ , it does not show a similar fall off as that of the  $\Sigma^+$  polarization. The model of hyperon polarization increasing linearly with  $P_t$  until  $P_t \sim 1$  GeV/c and then becoming constant<sup>9</sup> is not an adequate description of the  $\Sigma^+$  data presented here.

Data at 800 GeV are available for the  $\Xi^-$  system<sup>9</sup>. Both the  $\Xi^-$  and  $\Lambda^0$  measurements use a Be target as contrasted to the Cu target used by us. From these two studies we can select data in a similar region of  $P_t$  and compare the  $X_F$

dependence to our  $\Sigma^+$  measurements. These are plotted in Figures 2b and 2c. The fitted slopes are given in Table III. The effect of target materials has only been studied for the  $\Lambda^0$  system. In these studies target effects<sup>10</sup> were seen to be small. We assume that this is true for the other hyperons as well.

TABLE III. Polarization  $X_F$  Slopes.

Particle	Energy [GeV]	Ref	Target	$dP/dX_F$	
				$0.98 < P_t < 1.18$	$1.30 < P_t < 1.52$
$\Sigma^+$	800	this work	Cu	$1.11 \pm 0.36$	$0.31 \pm 0.12$
$\Lambda^0$	400	8	Be	$-0.66 \pm 0.07$	$-0.48 \pm 0.04$
$\Xi^-$	800	9	Be	$-0.01 \pm 0.06$	$-0.40 \pm 0.27$

The plots of Figure 2 show the differing behavior of the  $X_F$  dependence of the polarization for  $\Sigma^+$ ,  $\Lambda^0$ , and  $\Xi^-$  at two different values of  $P_t$ . In looking at the  $\Sigma^+$  and  $\Lambda^0$  plots one first notices that the signs of the polarizations are opposite. All models which incorporate the constituent quark picture are in agreement with this fact and also with the sign of the  $\Xi^-$  polarization. Taking into account the differing sign of the  $\Sigma^+$  and  $\Lambda^0$  polarizations, we see that their slopes,  $dP/dX_F$ , are of equal magnitude. In contrast the  $\Xi^-$  polarization is independent of  $X_F$ . In the constituent quark picture the  $\Sigma^+$  and  $\Lambda^0$  may contain two of the three incident proton quarks whereas in the  $\Xi^-$  case at most one of the proton quarks may be incorporated into the hyperon. This suggests that the mechanisms for producing the polarization may be very different. This hypothesis is supported by the observation of anti hyperon polarization<sup>1,11</sup>, where no constituent quarks are shared with the incident proton.

There is now a growing body of experimental data on hyperon inclusive polarization. In comparing the kinematical and particle dependence of hyperon polarization, we may gain insights into the underlying mechanisms responsible for the polarization. Why does the  $\Sigma^+$  polarization magnitude decrease beyond  $P_t \sim 1.0$  GeV/c whereas the  $\Lambda^0$  does not? Is there something unique about the  $\Sigma^+$ ? The magnitudes of the  $X_F$  dependence of hyperon polarization are similar for  $\Sigma^+$  and  $\Lambda^0$ . Is the fact that they differ from the  $\Xi^-$  dependence just a reflection of the



number of quarks transferred from the projectile to the hyperon? How are we to account for anti-hyperon polarization and the different energy dependencies of  $\Sigma^+$  and  $\Xi^-$  polarizations<sup>1,11</sup>? The only clear conclusion left in this field is that there are many more questions than answers.

We wish to thank the staffs of Fermilab and the Petersburg Nuclear Physics Institute for their assistance. This work is supported in part by the U.S. Department of Energy under contracts DE-AC02-76CH03000, DE-AC02-76ER03075, DE-FG02-91ER40631, DE-FG02-91ER40664, DE-FG02-91ER40682, the Russian Academy of Sciences, and the UK Science and Engineering Research Council.

- 
- (a) Graduate Student from CINVESTAV-IPN, Mexico; partially supported by CONACyT, Mexico.  
Now at the Super Collider Laboratory, Dallas, Texas 75237.
  - (b) Supported by FAPESP, Brazil
  - (c) Now At Fermilab
  - (d) Present address Department of Physics, University of Maryland, College Park, MD 20742
  - (e) Present address Department of Physics, University of California (Santa Cruz), Santa Cruz, CA, 95046.
  - (f) Present address *COPPE, Universidade Federal do Rio de Janeiro, Brazil*
  - (g) Partially supported by FAPESP and CNPq, Brazil
  - (h) Present address *Universidade de Sao Paulo, Sao Paulo, Brazil*
  - (i) Present address Department of Physics, Stanford University, Stanford, CA, 94309

### References

1. A. Morelos *et al.*, Phys. Rev. Lett. **71**, 2172(1993).
2. T.R. Cardello *et al.*, Phys. Rev. **32**, 1 (1985).
3. M. Foucher *et al.*, Phys. Rev. Lett. **68**, 3004 (1992).
4. A. Morelos *et al.*, Submitted to Phys. Rev. Lett. (1993).
5. A. Morelos, Ph.D. Thesis, Centro de Investigacion y de Estudios Avanzados del IPN, Mexico ,1992 (unpublished).
6. Particle Data Group, Phys. Rev. **D45**, 1 (1992).
7. G.L. Kane *et al.*, Phys. Rev. Lett. **41**, 1689 (1978).
8. B. Lundberg and *et al.*, Phys. Rev. **D40**, 3557 (1989).
9. J. Duryea *et al.*, Phys. Rev. Lett. **67**, 1193 (1991).
10. L. Pondrom Phys. Rep. **122**, 57 (1985).
11. P.M. Ho *et al.*, Phys. Rev. Lett. **65**, 1713 (1990).

## Figure Captions

1. Polarization for  $\Sigma^+$  as a function of  $P_t$  from this experiment.
2. Polarization of (a)  $\Sigma^+$ ; this work, (b)  $\Lambda^0$ ; ref 8, and (c)  $\Xi^-$ ; ref 9, as a function of  $X_F$  for two values values of  $P_t$ .

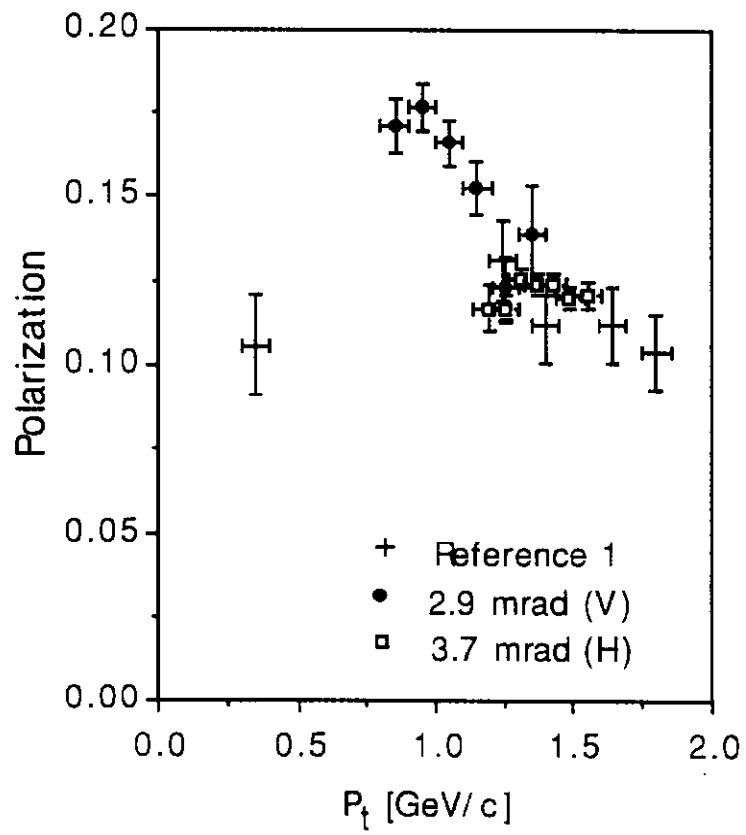


Figure 1

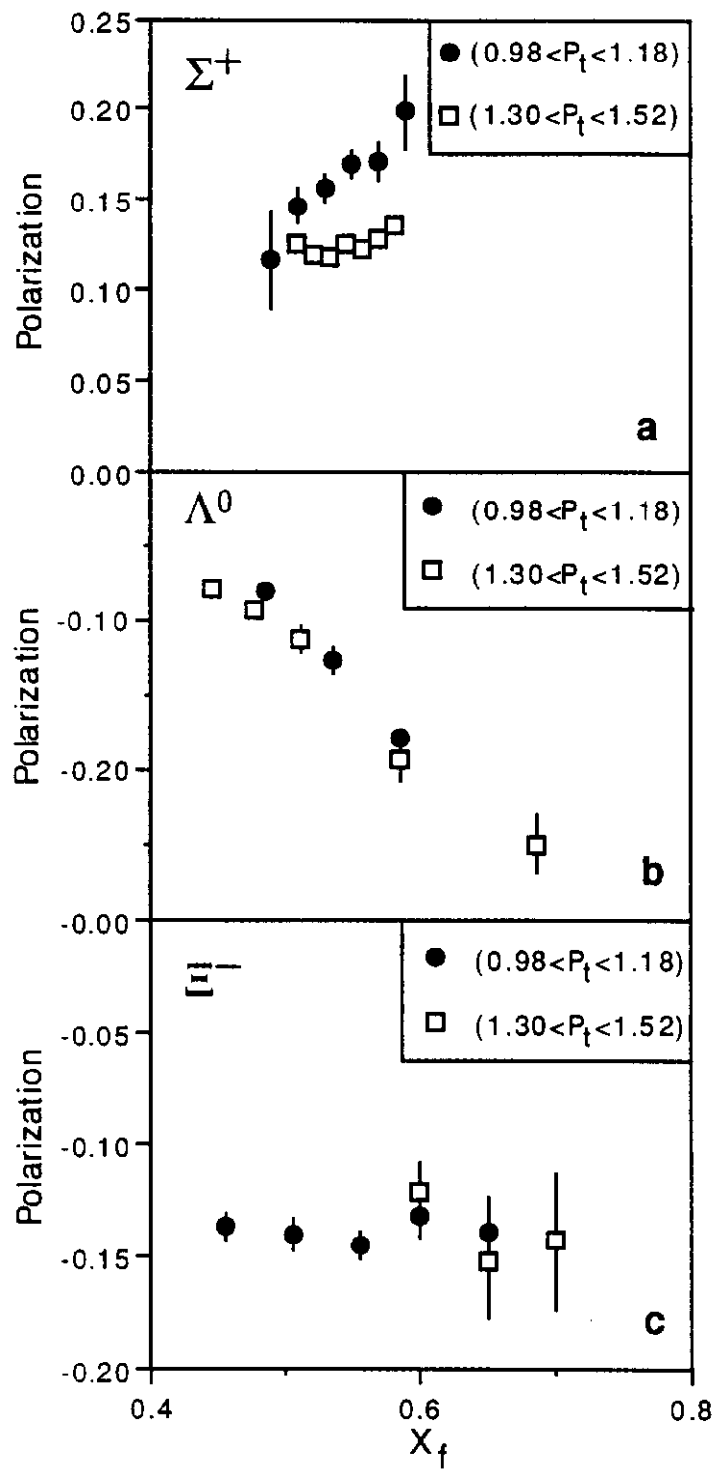


Figure 2